

Rec'd PCT/PTO 15 JUL 2004 #2

PCT/CA 03/002501

14 MAY 2003 14.05.03

PA 991052

REC'D 05 JUN 2003

WIPO PCT

THE UNITED STATES OF AMERICA

TO ALL TO WHOM THESE PRESENTS SHALL COME:

UNITED STATES DEPARTMENT OF COMMERCE

United States Patent and Trademark Office

April 08, 2003

THIS IS TO CERTIFY THAT ANNEXED HERETO IS A TRUE COPY FROM THE RECORDS OF THE UNITED STATES PATENT AND TRADEMARK OFFICE OF THOSE PAPERS OF THE BELOW IDENTIFIED PATENT APPLICATION THAT MET THE REQUIREMENTS TO BE GRANTED A FILING DATE UNDER 35 USC 111.

APPLICATION NUMBER: 60/362,590

FILING DATE: February 27, 2002

PRIORITY DOCUMENT
SUBMITTED OR TRANSMITTED IN
COMPLIANCE WITH
RULE 17.1(a) OR (b)

By Authority of the
COMMISSIONER OF PATENTS AND TRADEMARKS



M. K. Hawkins
M. K. HAWKINS
Certifying Officer

BEST AVAILABLE COPY

02/27/02
1165 U.S. PTO

Docket No. LAUZ-009

11011 U.S. PTO
60/362590
02/27/02

HONORABLE COMMISSIONER OF PATENTS AND TRADEMARKS

Sir:

Transmitted herewith for filing is the **provisional patent application** by the following named inventor(s):

| INVENTOR | RESIDENCE | CITIZENSHIP | MAILING ADDRESS |
|-----------------------|----------------------------------------------------|-------------|----------------------------------------------------|
| 1. Rhonda L. Millikin | 36 Ettrick Crescent Nepean, Ontario, K2J 1G1 | Canada | 36 Ettrick Crescent Nepean, Ontario, K2J 1G1 |

Applicant: Her Majesty the Queen in Right of Canada as Represented by the Minister
of National Defence
National Defence Headquarters
Ottawa, Ontario K1A 0K2
Canada

Enclosed are:

- ☐ Applicant Claims Small Entity Status. See 37 CFR 1.27.
☒ 21 pages of specification and abstract.
☐ Declaration and Power of Attorney
☒ 12 sheets of informal drawings.
☐ An assignment of the invention to _____ and the assignment
recordation fee.
☒ Large entity filing fee for a provisional application for patent: **\$160.00** (Check No. 12197)

Please send all communications to:

**Michael S. Neustel
Neustel Law Offices, LTD
2534 South University Drive, Suite No. 4
Fargo, North Dakota 58103**

Respectfully Submitted,


Michael S. Neustel, Reg. No. 41,221
2534 South University Drive, Suite No. 4

February 27, 2002
Date

11165 U.S. PTO
02/27/02

3-5-02

A/PR-V

Docket No. LAUZ-009

In The United States Patent & Trademark Office

In re Application of: **Her Majesty the Queen in Right of Canada as Represented by the Minister of National Defence**

Inventors: **Rhonda L. Millikin**

Filed: **U.S. Provisional Patent Application**

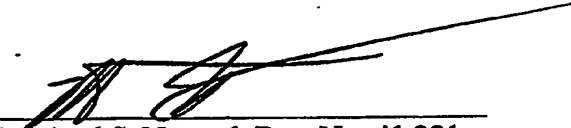
Express Mail Serial No.: **EV067206580US**

For: **Acoustic Location of a Stationary or Moving Source**

Date of Deposit: **February 27, 2002**

I hereby certify that the attached United States provisional patent application, formal drawings, transmittal letter are being deposited with the United States Postal Service under Express Mail service on the date indicated above and is addressed to:

**BOX PROVISIONAL PATENT APPLICATION
Commissioner of Patents
P.O. Box 2327
Arlington, VA 22202**


Michael S. Neustel, Reg. No. 41,221
2534 South University Drive, Suite No. 4
Fargo, ND 58103
(701) 281-8822

11011 U.S. PTO
60/362590
02/27/02

60362590-022702

FOR: U.S. PROVISIONAL APPLICATION FOR PATENT

TITLE: ACOUSTIC LOCATION OF A STATIONARY OR MOVING SOURCE

FIELD OF THE INVENTION

The present invention relates to an apparatus and method to locate an acoustic source. More specifically, the apparatus and method for acoustic location is based on the method of expanding hemispheres.

BACKGROUND OF THE INVENTION

Acoustic location of airborne targets is normally achieved using an analytic solution. For example, to passively monitor the acoustic location of a flying target like the night flight call of a migrant bird, an array of sensors (microphones) is used. The signals received from the sensors are calculated in time and space. The success of this method depends mainly on the number of microphones and geometry of the array of the microphones. Often, the accuracy of the results is diminished when a non-standard geometry is used or if the microphones cannot be adjusted to the same level.

One method of calculation is based on time difference of arrival (TDOA). In this case, two sensors will receive a signal from a distant source at different times. This difference in arrival times can be used to estimate the source's location (bearing and range). Referring to Figure 1, assuming far field conditions (i.e. planar wavefront not spherical) the target bearing is determined by the delay, $\Delta d_{21} = c\Delta t_{21} = x \cos\theta$, in the arrival of the wavefront at two time-synchronized sensors, R_1 and R_2 .

The angle θ is evaluated by equation (1)

$$\theta = \cos^{-1} (c\Delta t_{21}/x) \quad (1)$$

where Δt_{21} is the difference in seconds of the time of arrival of the acoustic signal at the two sensors, R_1 and R_2 .

2022010652909
The resulting θ and the geometry of the array define a hyperbolic surface of possible locations of the source. The hyperbolic surface is a continuum of points at the calculated angle and distance, in the plane perpendicular to the line joining R_1R_2 . Another two pairs of receivers are used to determine the hyperbolic surface with respect to each pair. Where these three hyperbolic surfaces intersect, defines the position of the acoustic source in 3-D.

The current TDOA calculation method is based on far field assumptions and hence is inaccurate for a near field situation as in the case of acoustic location of a bird in flight. In the near field situation, the source is assumed to be far enough away from the receivers (about 10 times greater than the distance between them) that the acoustic wavefronts can be assumed to be planar rather than the actual spherical shape. If far field assumptions are valid, Δt is calculated as shown in Figure 1. Otherwise, a near field situation occurs in which, Δt is calculated by acoustic reciprocity starting with spheres located at each microphone and expanding these spheres by the speed of sound towards the bird, until they intersect. A minimum of three TDOAs are required and therefore four microphones. To survey a sky large enough to find a bird when its location is not predictable, a large beam of acquisition is desired (60°). The radius of the microphone array will determine the height of intersection of the spheres and therefore, the potential sampling heights. A radius of 50 m provides a sampling height for landing birds 100-300 m.

It is therefore desired to have an apparatus and method for acoustic detection of a target in flight that can be accurate in a near field situation.

SUMMARY OF THE INVENTION

It is an object of the present invention to provide a method for determining the acoustic location of a target in flight that is in near a field situation. However, the method is not limiting to near field situations and may be used for far field situations, nor is the method limited to moving target.

Distinguishing features of the method of the present invention include the incorporation of wavelet analysis to allow for the Doppler shift of the entire acoustic signal, and the ability to accommodate non-standard

array geometries by using expanding spheres. For examples, non-standard includes uneven microphone heights, geometries of more than four microphones and without equilateral triangles.

Conventionally, beamforming is routinely used in antisubmarine warfare to localise a passive acoustic source. Location is determined by the phase relationships on arrival of a sound wave at an array of receivers. Beamforming therefore depends on frequency. For proper beamforming, the inter-microphone spacing, x , determines the maximum frequency of the source, f , that can be resolved according to equation (2):

$$x < \frac{c}{2f} \quad (2)$$

where c is the speed of sound. In the location of birds, if one uses $c = 340 \text{ m s}^{-1}$ and a maximum frequency for night flight calls of birds of 9 kHz, this method would limit the inter-microphone spacing to $< 2 \text{ cm}$.

This is undesirable and can be avoided using the time difference of arrival (TDOA) method. In this case, passive localisation of an emitting source involves intercepting the source signal at two or more microphones. The objective is to determine the source position.

Traditionally, position estimate is achieved using a minimisation procedure using the equations based on Figure 2a:

To locate an acoustic source, time difference of arrival (TDOA) or frequency difference of arrival (FDOA) can be used. In the case of night flight birds, due to the high frequency of their calls and the speed of sound in air, the required distance between receivers does not fit the dimensions of the standard microphones. This makes TDOA is the more useful method than beamforming.

Using TDOA, the location of the source can be obtained with straight cross-correlation analysis with, for example, a night flight call as the matched filter, or by visual inspection of recorded spectrograms. The use of wavelet analysis provides a more accurate correlation and thus, more accurate location than either of the

matched filter or spectrogram analysis approaches. However, the expanding sphere method of the present invention can make use of time differences obtained by all three approaches.

The determination of time differences using wavelet analysis differs from other approaches in that correlations are conducted using the matched filter as well as Doppler-shifted (compressed and stretched) forms of the matched filter. The shifted versions of the matched filter waveform are called baby wavelets and a bank or set of these baby wavelets is referred to as a wavelet bank. The recorded time series is compared with the wavelet bank to determine when the signal occurred in each channel. The match with a particular baby wavelet is more accurate because the frequency distortion of the received signal can be accommodated. Furthermore, by using a wavelet bank, the maximum correlation will indicate the velocity of the acoustic target as well as its location. After the match has been found the process is exactly comparable to other TDOA methods in that the relative time of the peak correlations provides the time difference, which is applied to the geometry of the microphone array. The present invention provides an easier method to deal with complex array geometries.

More specifically, the method of the present invention is based on the time difference of arrival (TDOA) calculation using acoustic reciprocity, i.e. procedure of expanding sphere or hemispheres. The procedure of expanding spheres of the present invention includes the following steps.

1. Given a valid (in terms of maximum distance the sound could travel and maximum speed of the target) set of TDOAs, a mesh of points is constructed on a unit sphere using the following definitions:

$$\theta = [-\pi \dots \theta_n \dots \pi] \quad (1 \times (n+1)) \text{ matrix} \quad (2)$$

$$\phi = \left[\frac{\pi}{2} \dots \phi_n \dots \frac{\pi}{3} \right] \quad ((n+1) \times 1) \text{ matrix} \quad (3)$$

$$\mathbf{O} = [1 \dots 1 \dots 1] \quad ((n+1) \times 1) \text{ matrix} \quad (4)$$

$$\mathbf{X} = \cos \phi \bullet \cos \theta \quad ((n+1) \times (n+1)) \text{ matrix} \quad (5)$$

$$\mathbf{Y} = \cos \phi \bullet \sin \theta \quad ((n+1) \times (n+1)) \text{ matrix} \quad (6)$$

$$\mathbf{Z} = \sin \phi \bullet \mathbf{O} \quad ((n+1) \times (n+1)) \text{ matrix} \quad (7)$$

where θ and ϕ are one dimensional matrices of $n+1$ points, $n = 200$ (minimum, more points for more accuracy), ϕ increases from the x axis and X, Y and Z are $(n+1)$ by $(n+1)$ matrices comprising the mesh of positions on the unit hemisphere (i.e., radius = 1). The elevation angle was restricted to $\pi/2$ to $\pi/3$ to focus the points within the maximum pickup region of the microphones. (note $\pi/3$ is the lower edge of the microphone beam for the microphones selected in this experiment. This value will depend on the particular microphone used and therefore could be more generally stated as the lower edge of the beam of acquisition)

2. Initialise the size of each sphere based on TDOA values from the correlation analysis:

$$\mathbf{X}_m(t_0) = D_m c \mathbf{X} \quad (8)$$

$$\mathbf{Y}_m(t_0) = D_m c \mathbf{Y} \quad (9)$$

$$\mathbf{Z}_m(t_0) = D_m c \mathbf{Z} \quad (10)$$

where m is the microphone number (i.e., 1 to 4 in the test case but this could be increased to any number of microphones desired, four is the minimum required for TDOA), D_m is the delay in arrival of the signal to each microphone based on the time of arrival at the closest microphone in seconds, c is the speed of sound determined by local meteorological conditions in $m s^{-1}$ and X,Y,Z were determined by the initial conditions defining a mesh on a spherical surface of unit radius (step 1). One D_m is 0, so initially one of the sets of equations is identically zero.

3. Place hemispheres at each microphone position according to the geometry of the PEPT acoustic array (i.e., each starting x, y, z position for the four microphones was positioned on the array):

$$(x_1, y_1, z_1) = (0, 0, 0) \quad (11)$$

$$(x_2, y_2, z_2) = (0, -50, 0) \quad (12)$$

$$(x_3, y_3, z_3) = (-50 \cos(\pi/6), 50 \sin(\pi/6), 0) \quad (13)$$

$$(x_4, y_4, z_4) = (50 \cos(\pi/6), 50 \sin(\pi/6), 0) \quad (14)$$

(note the geometry could be changed to any desired arrangement but the test case given here eliminates ambiguity over the centre of the array by having a central microphone and three outer microphones situated on an equilateral triangle).

4. Expand hemispheres in time intervals, t_i (s) with the growth of each hemisphere determined by c ($m s^{-1}$) based on local meteorological conditions:

$$r_{E,m}(t_i) = c(t + t_i + D_m) \quad (15)$$

$$\mathbf{X}_m(t_i) = r_{E,m}(t_i) \mathbf{X}_m \quad (16)$$

$$\mathbf{Y}_m(t_i) = r_{E,m}(t_i) \mathbf{Y}_m \quad (17)$$

$$\mathbf{Z}_m(t_i) = r_{E,m}(t_i) \mathbf{Z}_m \quad (18)$$

where D_m is the time delay at microphone m in seconds, c is the local speed of sound, $r_{E,m}$ is the radius at the expanded position or next time interval at microphone m in metres, $x_m(t_i)$, $y_m(t_i)$, $z_m(t_i)$ are new positions in metres based on the $r_{E,m}$ expansion at the t_i time interval, where $t_1 = 0.002$, and t is the time at the end of the previous step in s.

5. Search the matrix of points on each hemisphere for intersections:

$$XYZ_m = \begin{bmatrix} X_1 & Y_1 & Z_1 \\ M & M & M \\ X_{n+1} & Y_{n+1} & Z_{n+1} \end{bmatrix} \quad (19)$$

$$result = (x, y, z), \text{ where } XYZ_1 \cap XYZ_2 \cap XYZ_3 \cap XYZ_4 \quad (20)$$

6. Continue expanding hemispheres until there is an intersection between all hemispheres within an error region of 1 m^3 , or the hemispheres have grown beyond a maximum $t_i = 3 \text{ s}$ (note this could be increased if the target was expected to be higher than 1005 m). For the range of values of c at PEPT, this maximum limited the search to a radius of about 1000 m (e.g., with $c = 335 \text{ m s}^{-1}$, $335 \times 3 \text{ s} = 1005 \text{ m}$).

The intersection was found using a sub-routine of Matlab® that compares each row (in this case, each x , y , z) of a pair of matrices and outputs the set of rows common to both. The “result” is the intersection between the wavefronts initiated at microphone 1 and 2. This is then compared for overlapping locations with XYZ for microphone 3 and 4 and then again for any overlaps between those pairs.

The main advantage of the above method of expanding sphere is that it enables detection of a target in flight located in near field situation. This cannot be achieved with the current method of TDOA calculation, which is directed to far field situations, and therefore, assumes planar wavefronts.

The acoustic detection system and method of the present invention are applicable for detection of any moving or stationary target that emits a sound. This includes, for example, a bird, a plane, or a sniper. In

the latter case, the sniper can be located by the gunshot sound and further the bullet's trajectory can be determined.

In one aspect of the present invention, tracking and identification of the target in flight can be optimised by combining acoustic data with radar data. This can be accomplished by fusing acoustic and radar sensors to provide a complete system. In the case where the target is a bird, the radar can provide its flight speed, biomass and wing-beat characteristics; whereas the acoustic sensor can identify the species of birds.

BRIEF DESCRIPTION OF THE DRAWINGS

An embodiment of the present invention will now be described by way of examples with reference to the following drawings in which:

Figure 1 illustrates the target bearing procedure using time difference of arrival (TDOA) calculation;

Figure 2a is a schematic diagram showing the relationship between target and receiver array of microphones in prior art calculation of a target.

Figure 2 is a schematic diagram of the acoustic system of the present invention;

Figure 3 is a flow chart depicting the method for locating a target based on acoustic data of the present invention;

Figure 4a is a graph representing a segment of the calibration of time series obtained from example 1;

Figure 4 is a flow chart of the expanding sphere process of the present invention;

Figure 5 is a schematic diagram of a detection system of the present that includes a combination of acoustic and radar components;

Figure 6 is a flow chart depicting the calculation process using radar data to locate a target;

5

Figure 7 is a flow chart showing a method for detecting and tracking a target of the present invention based on acoustic and radar data.;

Figure 8 is a schematic diagram showing the geometry of the acoustic array used in experiment described in example 1;

Figure 9 is a schematic diagram showing the acoustic/radar set-up for the experiment described in example 2.

DETAILED DESCRIPTION OF THE PREFERRED EMBODIMENT

The present invention provides an acoustic system and method for acoustic tracking and location of a target in flight. Referring to Figure 2, a schematic diagram of the acoustic system is provided. The acoustic system includes an array of sensors or microphones connected to one another in a particular geometry. Preferably, the array has an equilateral shape with a central microphone. For example, using four microphones, a triangular array can be obtained by evenly spacing three microphones at 120° apart, and one microphone centrally positioned. This ensures that sound emitted directly over the array centre is captured. However, other geometries and additional microphones could be easily incorporated.

The microphones are further connected to a set of pre-amplifiers (not shown), digitiser, and a computer where digitised data can be stored. If the target emits a sound while flying above the array of sensors, it is captured, digitised and stored in the computer. Once the collection of acoustic data is completed, it is analysed to provide the location of the target. The analysis uses prior art TDOA wavelet calculation

method based on the procedure of expanding spheres of the present invention (Figure 3). The use of wavelet analysis is one novel aspect of the present invention.

Referring to Figure 3, acoustic field data are analysed as follows. The data is first correlated with the desired range of waveforms such as ballistic or bird waveforms. Data within the desired range are further analysed using TDOA. The TDOA procedure based on wavelet analysis, locates the target signal in each microphone channel via peaks in correlation between the received signal and a bank of wavelets which are Doppler shifted forms of the target signal at zero Doppler (stationary). Each time a peak correlation occurs in multiple channels, the time difference between reception of the same signal provides the data for TDOA analysis. These numbers are then submitted to the expanding hemisphere program.

The expanding sphere process includes the steps of

1. Given a valid set of TDOAs, a mesh of points is constructed on a unit hemisphere using the following definitions:

$$\theta = [-\pi \dots \theta_n \dots \pi] \quad (1 \times (n+1)) \text{ matrix} \quad (2)$$

$$\phi = \left[\frac{\pi}{2} \dots \phi_n \dots \frac{\pi}{3} \right] \quad ((n+1) \times 1) \text{ matrix} \quad (3)$$

$$\mathbf{O} = [1 \dots 1 \dots 1] \quad ((n+1) \times 1) \text{ matrix} \quad (4)$$

$$\mathbf{X} = \cos \phi \cdot \cos \theta \quad ((n+1) \times (n+1)) \text{ matrix} \quad (5)$$

$$\mathbf{Y} = \cos \phi \cdot \sin \theta \quad ((n+1) \times (n+1)) \text{ matrix} \quad (6)$$

$$\mathbf{Z} = \sin \phi \cdot \mathbf{O} \quad ((n+1) \times (n+1)) \text{ matrix} \quad (7)$$

where θ and ϕ are one dimensional matrices of $n+1$ points, $n = 200$ (exceptions given below), ϕ increases from the x axis and \mathbf{X} , \mathbf{Y} and \mathbf{Z} are $(n+1)$ by $(n+1)$ matrices comprising the mesh of positions on the unit hemisphere (i.e., radius = 1). The elevation angle was restricted to $\pi/2$ to $\pi/3$ to focus the points within the maximum pickup region of the microphones.

2. Initialise the size of each hemisphere based on TDOA values from the correlation analysis:

$$\mathbf{X}_m(t_0) = D_m c \mathbf{X} \quad (8)$$

$$\mathbf{Y}_m(t_0) = D_m c \mathbf{Y} \quad (9)$$

$$\mathbf{Z}_m(t_0) = D_m c \mathbf{Z} \quad (10)$$

where m is the microphone number (i.e., 1 to 4), D_m is the delay in arrival of the signal to each microphone based on the time of arrival at the closest microphone in seconds, c is the speed of sound determined by local meteorological conditions in $m s^{-1}$ and X, Y, Z were determined by the initial conditions defining a mesh on a spherical surface of unit radius (step 1). One D_m is 0, so initially one of the sets of equations is
 5 identically zero.

3. Place hemispheres at each microphone position according to the geometry of the PEPt acoustic array (i.e., each starting x, y, z position for the four microphones was positioned on the array):

$$(x_1, y_1, z_1) = (0, 0, 0) \quad (11)$$

$$(x_2, y_2, z_2) = (0, -50, 0) \quad (12)$$

$$(x_3, y_3, z_3) = (-50 \cos(\pi/6), 50 \sin(\pi/6), 0) \quad (13)$$

$$(x_4, y_4, z_4) = (50 \cos(\pi/6), 50 \sin(\pi/6), 0) \quad (14)$$

4. Expand hemispheres in time intervals, t_i (s) with the growth of each hemisphere determined by c (m s^{-1}) based on local meteorological conditions:

$$r_{E,m}(t_i) = c(t + t_i + D_m) \quad (15)$$

$$X_m(t_i) = r_{E,m}(t_i)X_m \quad (16)$$

$$Y_m(t_i) = r_{E,m}(t_i)Y_m \quad (17)$$

$$Z_m(t_i) = r_{E,m}(t_i)Z_m \quad (18)$$

where D_m is the time delay at microphone m in seconds, c is the local speed of sound, $r_{E,m}$ is the radius at the expanded position or next time interval at microphone m in metres, $x_m(t_i), y_m(t_i), z_m(t_i)$ are new positions in metres based on the $r_{E,m}$ expansion at the t_i time interval, where $t_i = 0.002$, and t is the time at the end of the previous step in s.

5. Search the matrix of points on each hemisphere for intersections:

$$XYZ_m = \begin{vmatrix} X_1 & Y_1 & Z_1 \\ M & M & M \\ X_{n+1} & Y_{n+1} & Z_{n+1} \end{vmatrix} \quad (19)$$

$$result = (x, y, z), \text{ where } XYZ_1 \cap XYZ_2 \cap XYZ_3 \cap XYZ_4 \quad (20)$$

6. Continue expanding hemispheres until there is an intersection between all hemispheres within an error region of $1 m^3$, or the hemispheres have grown beyond a maximum $t_i = 3$ s. For the range of values of
 30

c at PEPT, this maximum limited the search to a radius of about 1000 m (e.g., with $c = 335 \text{ m s}^{-1}$, $335 \times 3 \text{ s} = 1005 \text{ m}$).

The intersection was found using a sub-routine of Matlab® that compares each row (in this case, each x, y, z) of a pair of matrices and outputs the set of rows common to both. The "result" is the intersection between the wavefronts initiated at microphone 1 and 2. This is then compared for overlapping locations with XYZ for microphone 3 and 4 and then again for any overlaps between those pairs.

In one aspect of the present invention, the tracking and location of target in flight can be optimised by combining the acoustic system of the present invention with any radar system. Detection by an acoustic sensor requires the target to emit a sound signal, and hence combining the two systems enable silent target to be detected. Additionally, the range of detection for an acoustic sensor in atmosphere is less than a radar sensor. For example, the range of acoustic detection is less than 800 meters for night flight calls of nocturnal migrant birds using the microphones selected for the test case; whereas, it is greater than two kilometers for radar detection. It is noted that a longer acoustic range is possible but generally at the expense of volume of coverage. A larger volume of sky is preferable for targets like birds whose flight pattern cannot be predicted. This would also be true for other transient and unexpected targets e.g. ballistics.

In one embodiment of the invention, the acoustic/radar system is used to track birds in flight. For the purpose of tracking birds, the preferred radar system used is the modified marine radar described in US Patent Application 60/304,481, herein incorporated by reference. Briefly, the radar includes a modified antenna to enable determination of the bird's altitude. The antenna is modified by tilting its boresight to about 73° from the horizontal so that the lower half power point of the 26° beam is approximately 60° off the ground. The radar is connected to a digitiser and a recorder as shown in Figure 5. Figure 5 also shows how the acoustic and radar components are linked.

Data collected from the radar are analysed according to the process exemplified in Figure 6. The process involves detection, signal processing to form valid tracks and calculation of height of the final 3-D positioning along the track.

5 More particularly, the radar is calibrated according to standard procedures. The radar measurements are then converted from polar (r, θ, ϕ, t) to Cartesian (x, y, z, t) co-ordinates to enable combination thereof with those of the acoustic results. The geometric locations are also converted to geographic angles. Tracking is then performed using standard procedures. The tracks are then validated. For example, if the target is moving faster than) 33 m/s, then the data are discarded since birds do not typically fly that fast. The valid track data are then combined with, for example, meteorological data to provide velocity, bearing and height of the target. The velocity and bearing calculations are obtained using known methods, and the height measurements are obtained using the neutral regression method described in US Patent Application 60/304,481.

15 Briefly, the neutral regression method is based on the assumption that that when the target is directly overhead at its closest approach (CPA).

$$z_{\text{est}} = R_{\text{min}} \quad (21)$$

20 Where z_{est} is the estimated target height in meters, R_{min} is the minimum measured target range, i.e. CPA of the target in meters. Using this height estimate, x and y positions were generated for the entire track. When this assumption was not valid (i.e., the target was not directly above the radar), the position of the track at R_{min} was observed to deviate towards the radar location ($R_{\text{offset}} = 0$) from the otherwise straight sequence of positions. This apparent curving of tracks was noted by Cohen and Williams (1980) when birds were tracked at the upper edge of a surveillance radar antenna ($\geq 30^\circ$ above the radar in the usual horizontal orientation). They manually matched the curved track to a computer-generated family of curves.

If track curvature was observed in this thesis, the elevation angle was decreased in integer iterations from $\phi = 90^\circ$ to 59° thereby offsetting the radial distance (hence the name, R_{offset}). At each angle, a new track ($x, y,$

z) was computed until the track was straightened and closer in value to the proper height obtained. When the angle was iterated too far, the track was observed to bow out from the location of the radar.

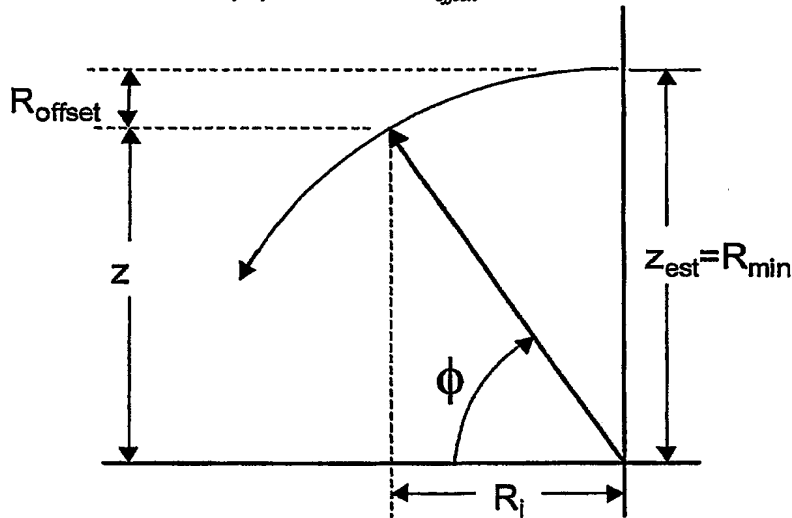
Neutral regression was used to select the track positions that best fit the main axis of the track. This fitting technique yields the orientation of the straight line that minimises the cross-line variance, assuming equal uncertainty in x and y (Pearson 1901).

The R_{offset} (range offset (m)) was the value used to correct the altitude and this was calculated from ϕ as follows.

1. Begin with the assumption that the target is at CPA of the radar ($\phi = 90^\circ$) and iterate through values of ϕ (deg), the elevation angle of the target with respect to the radar, from 90° to 59° . The operation was applied only at CPA.
2. Calculate R_{offset} values based on values of ϕ :

$$R_{offset_i} = R_{min} (\sin(90^\circ) - \sin(\phi_i)) \quad (22)$$

3. Calculate the corrected radius, R_i with values of R_{offset_i} :



3. Compute x, y, z at CPA. Apply that z to other positions along the track.
4. Calculate R_i based on z and R_{min} at each position.

$$R_i = \sqrt{R_{min}^2 - z^2} \quad (23)$$

5. Calculate the x, y co-ordinates based on R_i :

$$x_i = R_i \cos \theta_i \quad \text{and} \quad y_i = R_i \sin \theta_i \quad (24)$$

6. Conduct a neutral regression of each set of x, y points to find the set (defined by ϕ_i) that minimises the variance from the axis of the track. This value of ϕ is annotated ϕ_{opt} . (i.e., ϕ optimum).

5

7. Conduct a finer sweep using 0.1° increments in ϕ starting at $\phi_{opt}-1^\circ$ to $\phi_{opt}+1^\circ$, performing a regression at each increment until the optimum position is found (minimum length of the semi-minor axis of the principal ellipse).

10 The radar and acoustic data are analysed independently to, each, obtain a (x, y, z, t) tracks of the target. The radar data are then correlated with the acoustic data to locate overlapping data (Figure 7). The overlapping data confirm the true locations of the target, whereas the non-overlapping data are discarded. This does not mean the independent locations are incorrect. It means only that the target did not provide an acoustic signal while being tracked by the radar or a radar return while being detected acoustically.

15

Data within the desired range of waveforms are then analysed using TDOA. If the TDOAs do not make sense given the maximum distance between microphones and the maximum speed of the target then discard, otherwise the data is further analysed using the method of expanding sphere of the present invention (equations 2 to 20) to obtain an (x, y, z, t) location of the target.

20

The sensor fusion is not limited to radar. Rather, the acoustic method can provide target identification for other sensors such as infrared.

EXAMPLE 1

25 Acoustic Detection of a Known Moving Source

A cyclist rode past an acoustic array while continuously blowing a whistle. The array is shown in Figure 8. It has the source in one quadrant of the array, against a surveyed 20.13 m height above the array and R is the receiver.

5 Acoustic data collected from the sounds emitted by the whistle were analysed according to the method set out in Figure 3. This includes, namely, correlating the field data with whistle waveforms, thus filtering undesired sounds. The zero-Doppler waveform was recorded from a stationary source blowing into central microphone. This signal was then digitised and isolated. The whistle wavelet bank was then created by a sine function compression and expansion of the zero-Doppler (stationary) waveform of the whistle signal.

10 The data were then analysed using the time difference of arrival (TDOA) method based on wavelet analysis. Data that were not possible given the geometry of the microphone array and the speed of the target were discarded, and those that were within the expected speed of sound under the conditions of the experiment (temperature, wind, target flight behaviour) were further analysed using the method of
15 expanding spheres of the present invention (equations 2-20, Figure 4).

By graphing the magnitude of the correlation between the signal and wavelet bank, on a plot of the scale of the Doppler-shifted wavelets versus time, the slope of high correlation ridges indicated the direction the target was moving relative to the microphones as shown in Figure 4a. Figure 4a represents a segment of
20 the calibration time series when a cyclist passing by the acoustic array blew a whistle ($f_0=3\text{kHz}$, sampling rate= 44kHz). The whistle arrived at Channel 1, 3, 2 and 4. The arrows mark the positions used to calculate TDOA. Magnitude of the convolution is represented by colour brightness with yellow>red>blue.

When the target approached the microphone, the slope was negative. The slope was infinite as the target
25 went overtop of the microphone, and negative as the target passed the microphone. This provides a more accurate TDOA for location of the target than straight matched filter correlation analysis. The location with the matched filter would be difficult as the proper correlation peak could be any yellow along the line

through scale = 1.0. Note especially, that the correlation value at CPA (indicated by the arrow) would be misleadingly low (less intense in colour).

The scale of the wavelet which was maximally correlated with the signal, gave a measure of the velocity of the target relative to the receiver. In the test case using a cyclist travelling at a known speed, the wavelet analysis confirmed this speed (i.e., scale conversions gave relative velocities of -5.8 m s^{-1} , -7.8 m s^{-1} and 13.8 m s^{-1} . The cyclist's reported speedometer reading was 5.6 to 13.9 m s^{-1}).

The scale provides further information on the target position (up or down Doppler) relative to each microphone (negative velocities so approaching microphones 1, 2 and 4; and positive velocity so leaving microphone 3), and therefore, direction of movement. The direction of the cyclist was also confirmed by segmenting the recorded time series and calculating the change in position over one second interval of the ten seconds time series. The cyclist was correctly determined to be moving east-south-east (110°) (Figure 8).

EXAMPLE 2

Detection of Birds Using Acoustic/Radar System

Swainson's thrush (SWTH) and zeep nocturnal migrant birds were used to demonstrate the capability of the acoustic/radar system.

The experiment was conducted at Prince Edward Point (PEPt), Picton Country ($43^\circ 56' 00'' \text{N}$, $76^\circ 52' 00'' \text{W}$, $43^\circ 45' 30'' \text{N}$, $76^\circ 51' 45'' \text{W}$) because nocturnal migrants are known to land there in large numbers. The site is relatively open, quiet, protected from human interference, and provided landing habitat for nocturnal migrants. The acoustic/radar set-up is represented in Figure 9.

Sampling was divided into three time periods: dusk, midnight and dawn. Target behaviour at dawn was expected to be significantly different from the other two time periods. At dawn, the flight of landing birds

were expected to be reduced in altitude and opposite the mean flight direction of birds sampled at midnight. Birds at dusk were expected to climb in height and fly grouped in the same general direction as midnight targets. As the exact timing of the onset of landing was not known, sampling began one hour before dawn. Radar and acoustic samples were collected simultaneously for one hour for all three times periods.

5

The collected radar data were analysed according to the method shown in Figure 6 to provide the results in Table 1.

202201060952590.022702

Table 1: Locations of SWTH and ZEEP Targets Based on Radar Data

| Date | Period | Returns ^a | Intensity ^b | Int_SD | Speed ^c | Sp_SD | Altitude ^d | Alt_SD | n | Direction ^e | H _s ^f | E _H ^g |
|----------|-----------|----------------------|------------------------|--------|--------------------|-------|-----------------------|--------|----|------------------------|-----------------------------|-----------------------------|
| 28-Aug | Dawn | 4.3 | 196 | 17.2 | 10 | 3.6 | 237 | 57.9 | 19 | SE | 2.254 | 0.979 |
| 29-Aug | Dusk | 3.6 | 222 | 17.4 | 21 | 6.1 | 256 | 143.8 | 19 | SE | | |
| | Midnight | 4.1 | 216 | 19.5 | 14 | 2.9 | 227 | 88.3 | 17 | SE | | |
| 12-Sep | Dawn | 4.2 | 199 | 15.2 | 20 | 12.7 | 270 | 78.3 | 18 | SW | 2.413 | 0.941 |
| | Dusk | 3.5 | 210 | 19.2 | 18 | 8.3 | 258 | 122.9 | 34 | SE | | |
| | Midnight | 3.1 | 238 | 11.7 | 19 | 9.5 | 188 | 36.3 | 41 | SW | | |
| 18-Sep | Dawn | 6.3 | 213 | 18.1 | 16 | 8.2 | 229 | 61.3 | 39 | SW | 2.28 | 0.917 |
| | Dawn | 3.6 | 222 | 18.6 | 19 | 8 | 277 | 79.7 | 49 | SW | 2.548 | 0.774 |
| 19-Sep | Dawn | 3.8 | 172 | 14.3 | 18 | 8.4 | 193 | 52.4 | 41 | NW | 2.691 | 0.884 |
| All days | All times | 3.9 | 210 | 16.8 | 17 | 7.5 | 237 | 80.1 | 31 | SW | 3.758 | 0.993 |

5 ^a average number of pulse returns per track

^b average intensity of radar pulse return (\pm SD in next column)

^c average (\pm SD in next column) of all tracks during the sampling period and date in m s⁻¹

^d average (\pm SD in next column) of all tracks during the sampling period and date in m

^e quadrant including most track directions (NE,SE,SW or NW)

10 ^f Shannon diversity index (H_s) (Appendix C.7, Table C-4)

^g Shannon's equitability (Appendix C.7, Table C-4)

15 The acoustic data were analysed according to the method shown in Figure 3 to provide the results in Table

2.

20220106529E09

Table 2: Locations of SWTH and ZEEP Targets Based on Acoustic Data

| Date | Time of nfc ^a | Species | x (m) | y (m) | z (m) | Vel.(m/s) ^b | Range (m) | Azimuth (deg) |
|---------------------|--------------------------|-----------------------------------------------------------------------------------------------|-------|-------|-------|------------------------|-----------|---------------|
| 29 Aug ^c | 5:02:18:227 | zeep | -104 | -99.6 | 100 | 10.6 | 175 | 136 |
| | 5:05:49:806 | zeep | -348 | -14 | 438 | 33.7 | 559 | 178 |
| | 5:05:49:993 | zeep | -25.6 | -3.6 | 690 | 33.7 | 692 | 172 |
| | 5:11:37:085 | swth | -71.6 | -41.6 | 1016 | 9.9 | 1019 | 150 |
| | 5:11:51:309 | zeep | -65 | 37.5 | 154 | 22.7 | 97 | 230 |
| | 5:12:59:503 | swth | -35.6 | 0.4 | 366 | 3.7 | 368 | 181 |
| | 5:14:18:638 | swth | 48.4 | -29.6 | 750 | 18.7 | 752 | 32 |
| | 5:14:20:196 | swth | -65.6 | -3.6 | 78 | 5.8 | 102 | 177 |
| | 5:14:43:733 | zeep | -9.6 | 6.4 | 146 | 8.9 | 147 | 214 |
| | 5:14:43:943 | zeep | -35.6 | 16.4 | 148 | 8.9 | 153 | 205 |
| 18 Sep ^d | 5:35:37:011 | swth | -7 | 3 | 69 | 5.8 | 76 | 179 |
| | 5:02:08:409 | swth | -18 | 12 | 79 | 36.4 | 91 | 191 |
| | 5:02:10:775 | swth | -46 | 28 | 81 | 33.7 | 111 | 199 |
| | 5:02:11:227 | swth | -44 | 24 | 96 | 36.4 | 120 | 196 |
| | 5:08:34:349 | swth | 44 | -26 | 70 | 14.2 | 78 | 58 |
| | 5:08:35:248 | zeep | -43 | -25 | 65 | 14.2 | 99 | 157 |
| | 5:15:30:772 | swth | 26 | -10 | 100 | 16.5 | 101 | 88 |
| | 5:19:04:308 | zeep | -268 | 236 | 220 | 25.9 | 439 | 218 |
| | 5:19:05:947 | swth | 6 | 47 | 124 | 10.6 | 192 | 246 |
| | 5:32:33:460 | swth | 101 | -6 | 103 | 12.0 | 128 | 7 |
| | 5:39:27:226 | swth | 9 | -4 | 94 | 16.5 | 96 | 155 |
| | 5:39:51:112 | swth | 20 | -52 | 81 | 18.7 | 98 | 96 |
| | 5:39:51:644 | swth | 16 | -24 | 76 | 14.2 | 81 | 109 |
| | 5:39:52:825 | zeep | 10 | -6 | 68 | 10.6 | 70 | 148 |
| | 5:39:55:197 | swth | 50 | 49 | 78 | 21.1 | 94 | 298 |
| | 5:41:31:123 | swth | -25 | 7 | 105 | 23.5 | 117 | 184 |
| | 5:41:34:784 | zeep | 19 | -23 | 155 | 28.5 | 157 | 104 |
| | 5:41:37:557 | zeep | -28 | 61 | 71 | 28.5 | 106 | 227 |
| | 5:41:37:901 | swth | -23 | -14 | 69 | 16.5 | 88 | 160 |
| | 5:42:24:331 | zeep | 38 | -1 | 81 | 25.9 | 82 | 20 |
| | 5:42:25:387 | zeep | 0 | -27 | 185 | 23.5 | 188 | 130 |
| | 5:42:26:113 | zeep | 0 | 47 | 69 | 23.5 | 85 | 240 |
| | 5:42:26:582 | swth | -15 | -9 | 60 | 9.9 | 74 | 163 |
| | 5:42:26:605 | swth | 0 | 192 | 141 | 18.4 | 237 | 262 |
| | 5:42:33:561 | swth | 0 | -1 | 65 | 0.0 | 70 | 170 |
| | 5:42:35:274 | swth | -35 | -21 | 67 | 10.6 | 94 | 158 |
| | 5:42:35:367 | swth | 0 | 0 | 69 | 3.7 | 74 | 172 |
| | 5:42:35:749 | zeep | 0 | -1 | 68 | 25.9 | 73 | 170 |
| | 5:42:37:208 | swth | 25 | 14 | 79 | 5.4 | 80 | 267 |
| | 5:57:09:902 | zeep | 20 | 6 | 78 | 14.2 | 78 | 203 |
| | | same species | | | | | | |
| | | both species | | | | | | |
| | | ^a Time of night flight call (hour:min:sec:msec) ^c proportion zeep = 55% | | | | | | |
| | | ^b Maximum absolute value ^d proportion SWTH = 62% | | | | | | |

The two sets of data were then correlated to locate overlapping data. The overlapping data confirms locations of the targets (Table 3).

Table 3: Locations of SWTH and ZEEP Targets Based on Acoustic/Radar Data Fusion

5

| Date | Period | Parameter | Radar Track Positions | | | | | Acoustic Loc | Sync Bias ° | Data Fusion | | | |
|--------|--------|----------------------|-----------------------|---------|---------|---------|---------|--------------|---------------|-------------|-----------|-----------|--------|
| | | | 1 | 2 | 3 | 4 | 5 | | | Species | Vel (m/s) | Dir (deg) | Ht (m) |
| 12-Sep | Dawn | Time | 5:05:30 | 5:05:33 | 5:05:35 | 5:05:37 | | 5:05:50 | 50 - 38 = 14 | zeep | 11 | 254 | 435 |
| | | Range ^a | 413 | 435 | 435 | 443 | | 435 | | | | | |
| | | Azimuth ^b | 73 | 83 | 88 | 95 | | 89 | | | | | |
| 12-Sep | Dawn | Time | 5:34:29 | 5:34:32 | 5:34:34 | | | 5:34:37 | 37 - 27 = 10 | swth | 10 | 45 | 488 |
| | | Range ^a | 510 | 495 | 488 | | | 640 | | | | | |
| | | Azimuth ^b | 165 | 162 | 160 | | | 172 | | | | | |
| 18-Sep | Dawn | Time | 5:13:59 | 5:14:01 | 5:14:04 | 5:14:08 | | 5:14:08 | 8 - 0 = 8 | swth | 15 | 225 | 98 |
| | | Range ^a | 180 | 165 | 150 | 150 | | 140 | | | | | |
| | | Azimuth ^b | 358 | 340 | 320 | 303 | | 358 | | | | | |
| 18-Sep | Dawn | Time | 5:17:54 | 5:17:56 | 5:17:58 | 5:18:01 | 5:18:03 | 5:18:04 | 64 - 55 = 9 | zeep | 12 | 252 | 218 |
| | | Range ^a | 218 | 225 | 240 | 255 | 285 | 203 | | | | | |
| | | Azimuth ^b | 210 | 215 | 220 | 223 | 225 | 214 | | | | | |
| 18-Sep | Dawn | Time | 5:40:55 | 5:40:58 | 5:41:02 | | | 5:40:28 | 28 - 59 = -33 | swth | 7 | 292 | 83 |
| | | Range ^a | 150 | 157 | 195 | | | 188 | | | | | |
| | | Azimuth ^b | 255 | 262 | 270 | | | 262 | | | | | |
| 19-Sep | Dawn | Time | 5:07:06 | 5:07:10 | 5:07:13 | 5:07:15 | | 5:07:09 | 9 - 18 = -7 | swth | 37 | 120 | 161 |
| | | Range ^a | 188 | 285 | 315 | 435 | | 473 | | | | | |
| | | Azimuth ^b | 65 | 63 | 85 | 93 | | 92 | | | | | |
| 19-Sep | Dawn | Time | 5:11:02 | 5:11:05 | 5:11:07 | | | 5:11:13 | 13 - 3 = 10 | thrush | 18 | 352 | 165 |
| | | Range ^a | 165 | 158 | 173 | | | 188 | | | | | |
| | | Azimuth ^b | 60 | 70 | 113 | | | 63 | | | | | |
| 19-Sep | Dawn | Time | 5:11:07 | 5:11:09 | 5:11:12 | 5:11:14 | | 5:11:13 | 13 - 10 = 3 | thrush | 25 | 187 | 135 |
| | | Range ^a | 188 | 180 | 173 | 165 | | 270 | | | | | |
| | | Azimuth ^b | 225 | 233 | 238 | 285 | | 214 | | | | | |
| 19-Sep | Dawn | Time | 5:11:16 | 5:11:19 | 5:11:21 | 5:11:23 | | 5:11:23 | 23 - 18 = 5 | swth | 13 | 347 | 143 |
| | | Range ^a | 158 | 158 | 150 | 143 | | 90 | | | | | |
| | | Azimuth ^b | 100 | 78 | 68 | 65 | | 94 | | | | | |
| 19-Sep | Dawn | Time | 5:11:26 | 5:11:28 | 5:11:30 | | | 5:11:24 | 24 - 23 = 3 | swth | 26 | 62 | 293 |
| | | Range ^a | 293 | 300 | 308 | | | 360 | | | | | |
| | | Azimuth ^b | 330 | 340 | 350 | | | 313 | | | | | |
| 19-Sep | Dawn | Time | 5:28:43 | 5:28:50 | | | | 5:28:43 | 43 - 47 = -4 | thrush | 15 | 318 | 113 |
| | | Range ^a | 153 | 153 | | | | 143 | | | | | |
| | | Azimuth ^b | 75 | 20 | | | | 36 | | | | | |

^a in m (1 bin = 7.5m)
^b in deg (1 bin = 0.5 deg)
^c time of acoustic location minus time on radar track in seconds
* estimated timing of acoustic signal

Tables 1, 2 and 3 show a variety of birds, which demonstrate that the invention works for a large range of bird types.

10

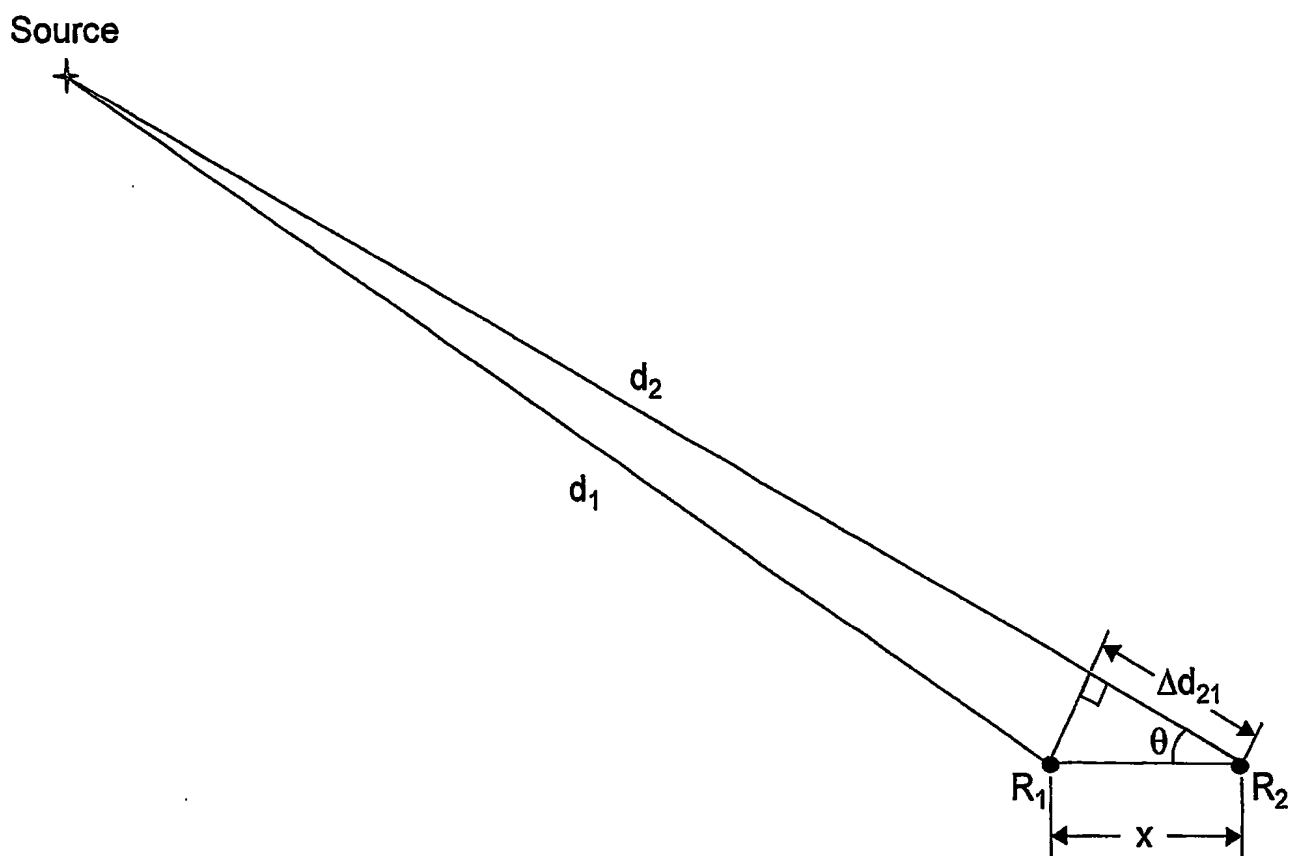
While the foregoing embodiment of the present invention have been described and shown, it is understood that all alternatives and modifications may be made and fall within the scope of the invention.

ABSTRACT

A method of acoustic location of a stationary or moving source is disclosed. The method is based on the time difference of arrival (TDOA) calculation using acoustic reciprocity, i.e. procedure of expanding
5 spheres or hemispheres. A detection system is also disclosed, which includes the combination of acoustic and radar detection apparatus.

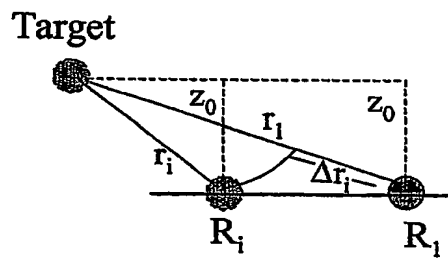
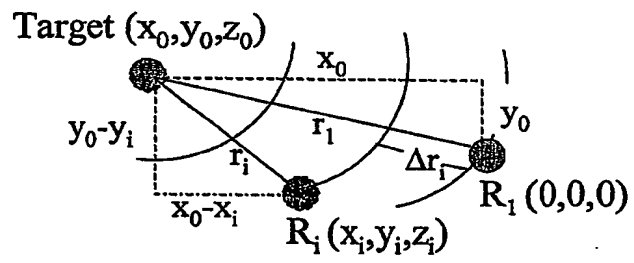
20220106529E09

FIGURE 1
(PRIOR ART)



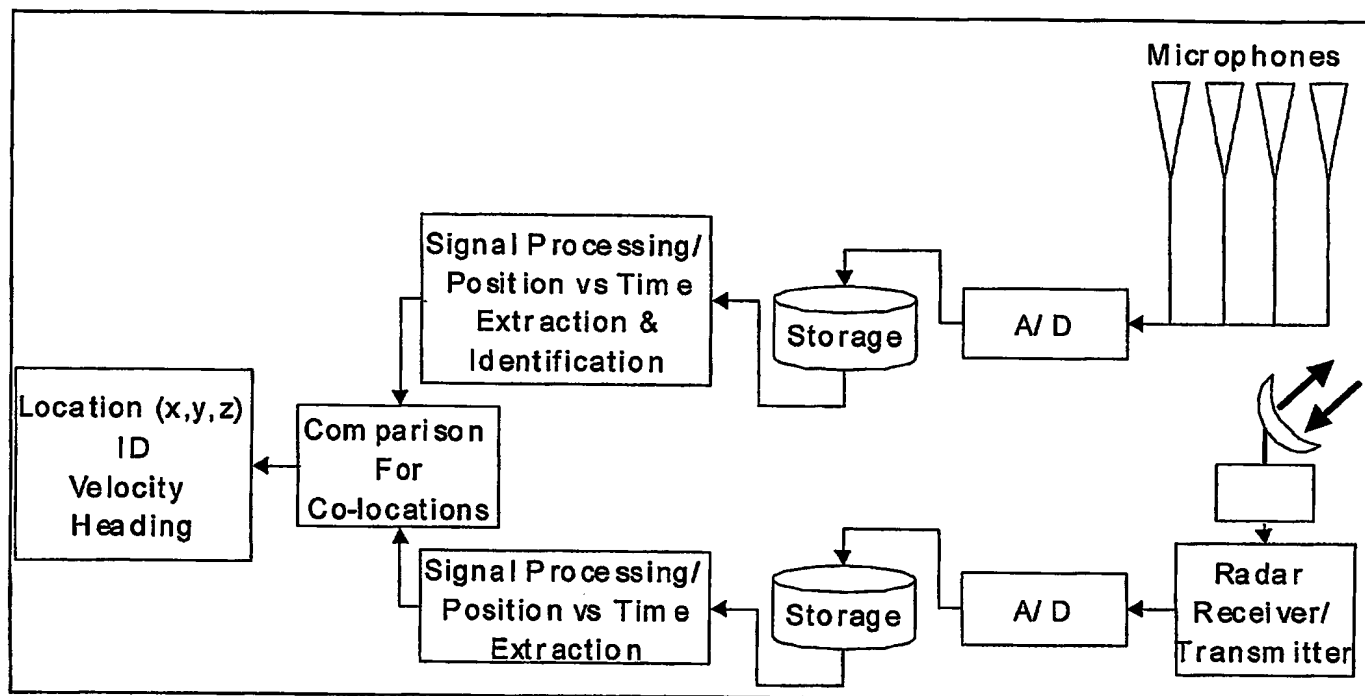
20220706529E09

FIGURE 2A



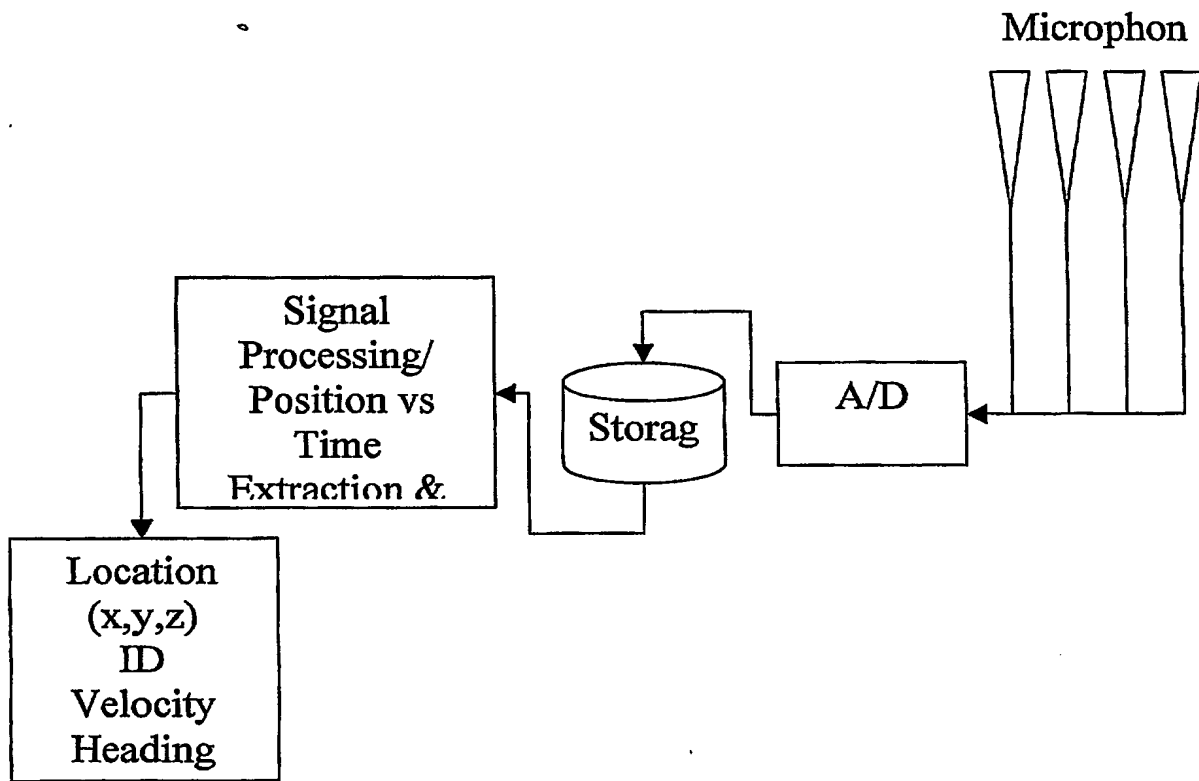
60362590.022702

FIGURE 2



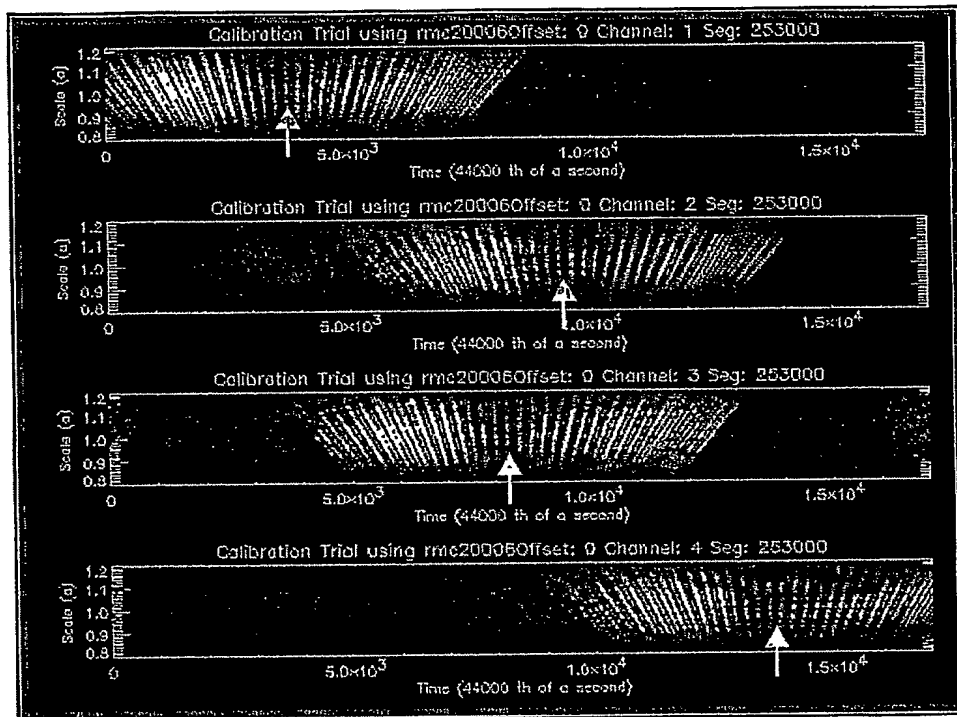
20.220.0659509

FIGURE 3



20220206 05525909

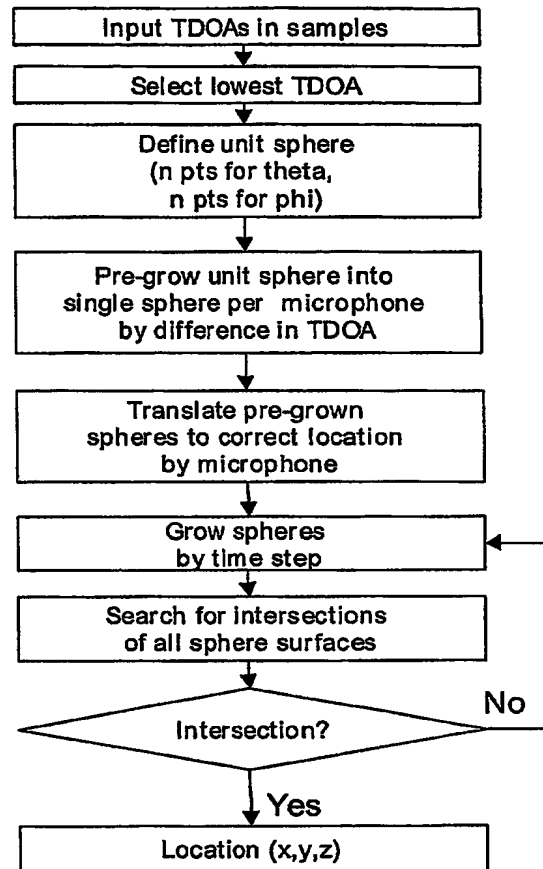
FIGURE 4a



(Black and White Version)

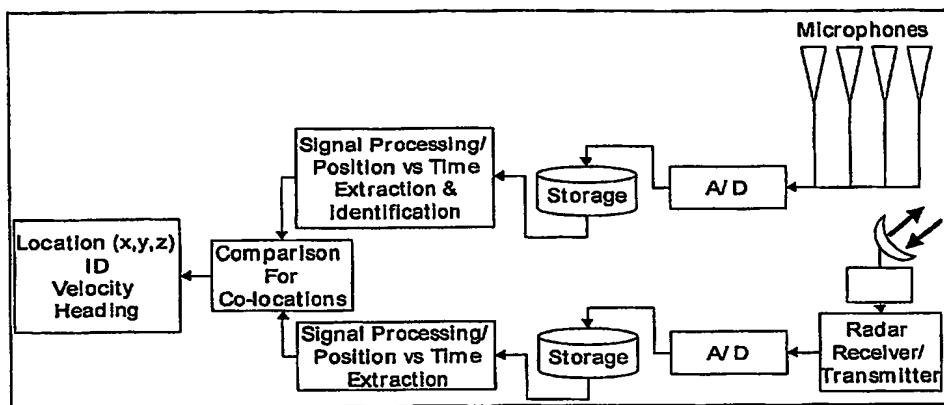
BEST AVAILABLE COPY

FIGURE 4



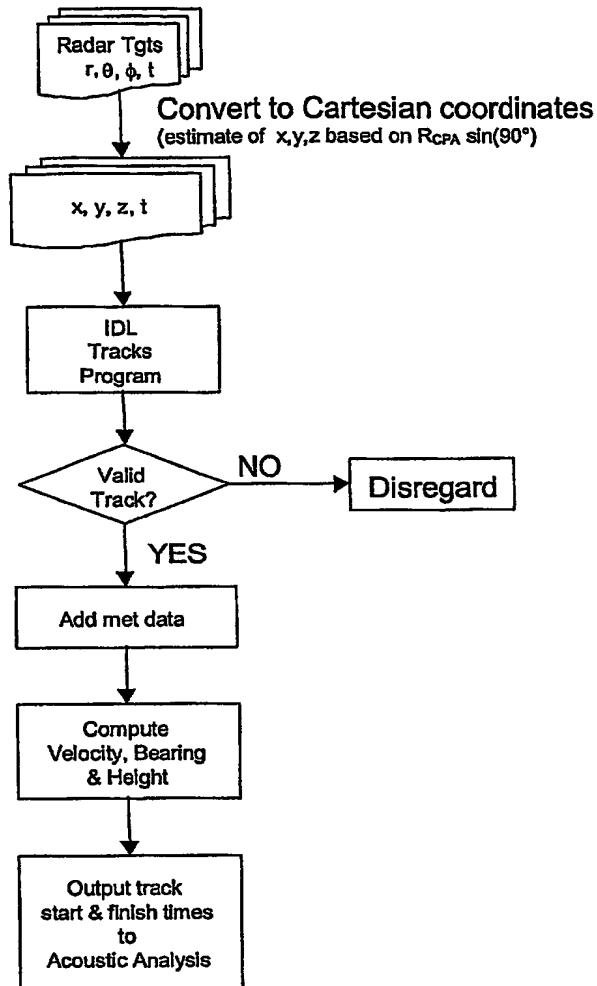
2022010652909

FIGURE 5



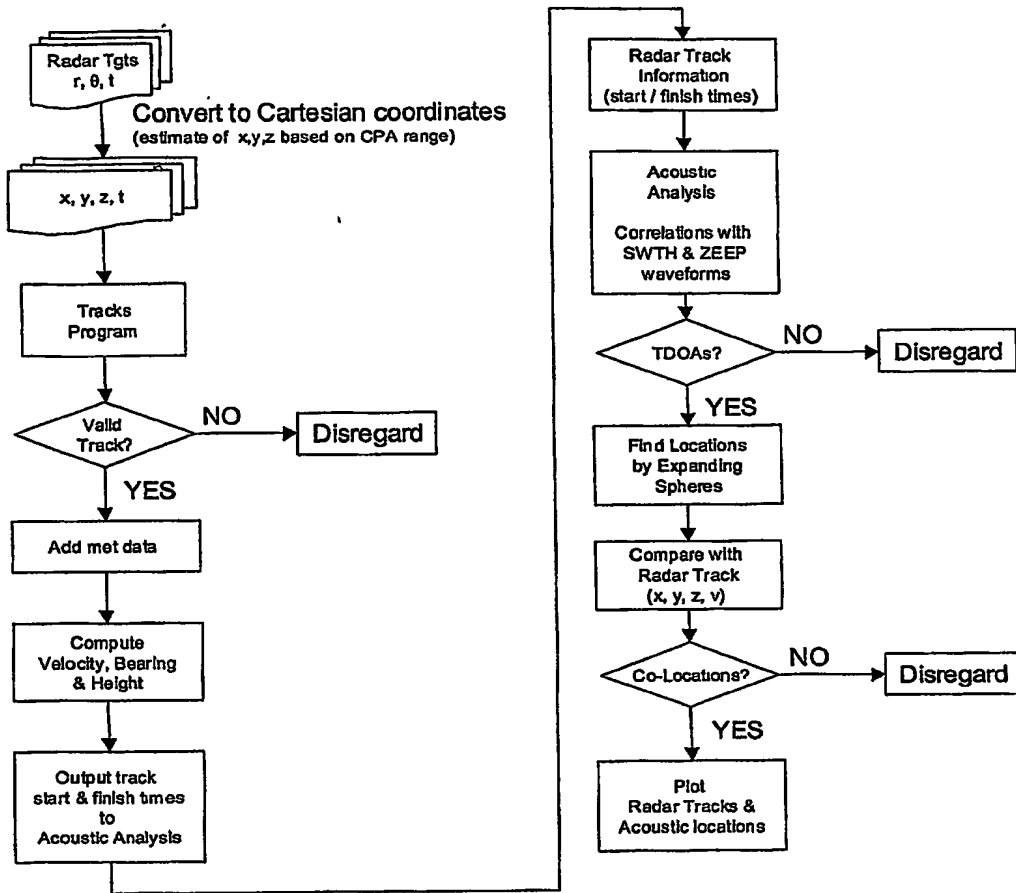
2022062909:022702

FIGURE 6



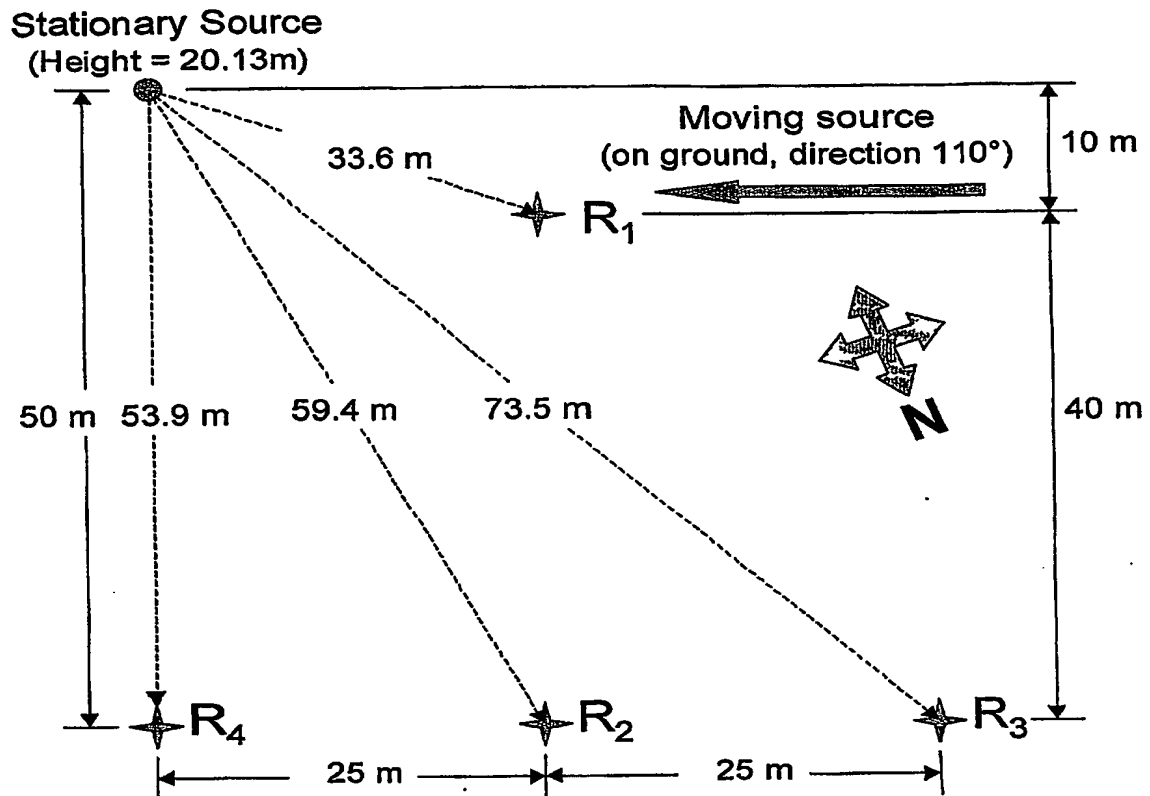
20220106090909

FIGURE 7



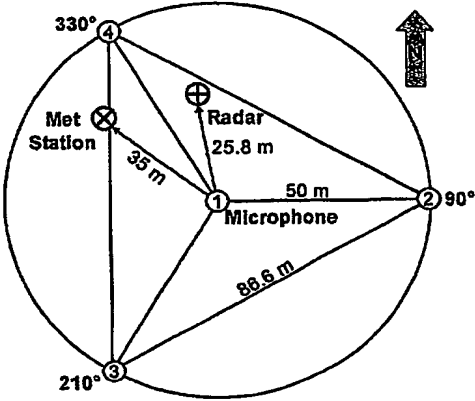
202206290002

FIGURE 8



20220106529E09

FIGURE 9



20220706090909

United States Patent & Trademark Office
Office of Initial Patent Examination

Application papers not suitable for publication

SN 60362590

Mail Date 02.27.02

- ☐ Non-English Specification
- ☒ Specification contains drawing(s) on page(s) _____ or table(s) _____
- ☐ Landscape orientation of text ☐ Specification ☐ Claims ☐ Abstract
- ☐ Handwritten ☐ Specification ☐ Claims ☐ Abstract
- ☐ More than one column ☐ Specification ☐ Claims ☐ Abstract
- ☐ Improper line spacing ☐ Specification ☐ Claims ☐ Abstract
- ☐ Claims not on separate page(s)
- ☐ Abstract not on separate page(s)
- ☐ Improper paper size -- Must be either A4 (21 cm x 29.7 cm) or 8-1/2"x 11"
- ☐ Specification page(s) _____ ☐ Abstract
- ☐ Drawing page(s) _____ ☐ Claim(s)
- ☐ Improper margins
- ☐ Specification page(s) _____ ☐ Abstract
- ☐ Drawing page(s) _____ ☐ Claim(s)
- ☐ Not reproducible Section
- Reason ☐ Specification page(s) _____
- ☐ Paper too thin ☐ Drawing page(s) _____
- ☐ Glossy pages ☐ Abstract
- ☐ Non-white background ☐ Claim(s)
- ☐ Drawing objection(s)
- ☐ Missing lead lines, drawing(s) _____
- ☐ Line quality is too light, drawing(s) _____
- ☐ More than 1 drawing and not numbered correctly
- ☐ Non-English text, drawing(s) _____
- ☐ Excessive text, drawing(s) _____
- ☐ Photographs capable of illustration, drawing(s) _____

60362590-022702

**This Page is Inserted by IFW Indexing and Scanning
Operations and is not part of the Official Record**

BEST AVAILABLE IMAGES

Defective images within this document are accurate representations of the original documents submitted by the applicant.

Defects in the images include but are not limited to the items checked:

- ☐ **BLACK BORDERS**
- ☐ **IMAGE CUT OFF AT TOP, BOTTOM OR SIDES**
- ☒ **FADED TEXT OR DRAWING**
- ☒ **BLURRED OR ILLEGIBLE TEXT OR DRAWING**
- ☐ **SKEWED/SLANTED IMAGES**
- ☐ **COLOR OR BLACK AND WHITE PHOTOGRAPHS**
- ☐ **GRAY SCALE DOCUMENTS**
- ☒ **LINES OR MARKS ON ORIGINAL DOCUMENT**
- ☐ **REFERENCE(S) OR EXHIBIT(S) SUBMITTED ARE POOR QUALITY**
- ☐ **OTHER:** _____

IMAGES ARE BEST AVAILABLE COPY.

As rescanning these documents will not correct the image problems checked, please do not report these problems to the IFW Image Problem Mailbox.